Science Advances

AAAS

advances.sciencemag.org/cgi/content/full/2/10/e1600492/DC1

Supplementary Materials for

Virus-mediated archaeal hecatomb in the deep seafloor

Roberto Danovaro, Antonio Dell'Anno, Cinzia Corinaldesi, Eugenio Rastelli, Ricardo Cavicchioli, Mart Krupovic, Rachel T. Noble, Takuro Nunoura, David Prangishvili

Published 12 October 2016, *Sci. Adv.* **2**, e1600492 (2016)
DOI: 10.1126/sciadv.1600492

This PDF file includes:

- References (*51–71*)

Supplementary Methods

Total prokaryotic abundance and biomass. Filters were stained with 20 µl of SYBR Green I (10000× stock) diluted 1:20 in pre-filtered TE buffer (10 mM Tris-HCl, 1 mM EDTA, pH 7.5), with excess stain removed 3 times using 3 ml of Milli-Q water, and mounted onto microscope slides (*51*). At least 20 microscope fields and 400 cells were counted randomly using epifluorescence microscopy with blue excitation. For the determination of the prokaryotic biomass, prokaryotic size was converted into bio-volume following inter-calibration with Scanning Electron Microscope (SEM) based size determinations (*5*, *52*).

Quantification of bacteria and archaea by catalysed reporter deposition fluorescence in situ hybridization (CARD-FISH). Sediment samples were washed with phosphate-buffered saline (PBS) (145 mM NaCl, 1.4 mM NaH_2PO_4, 8 mM Na_2HPO_4; pH 7.6), centrifuged and suspended in 1:1 solution of PBS:96% ethanol. After sonication, samples were diluted, filtered onto 0.2-µm filters and dipped in low-gellingpoint agarose (0.1% (wt/vol) in Milli-Q water), dried on Petri dish at 37°C, and dehydrated in 95% ethanol. Cell wall permeabilization was optimized by incubation at 37°C with lysozyme for bacteria or proteinase K for archaea (*36*, *53*). After Milli-Q washing and incubation in 10 mM HCl (room temperature, 20 min) the filters were then washed again, dehydrated in 95% ethanol, dried and hybridized with oligonucleotide Horseradish Peroxidase (HRP)-labeled probes Eub-mix (Eub338, Eub338-II and Eub338-III) targeting Bacteria, and Arch915 targeting Archaea. The absence of nonspecific signals was routinely checked using the NON-338 probe. Hybridization (35°C for Bacteria, 46°C for Archaea) was performed for 2 hours. Then the filters were transferred into preheated washing buffer, placed in PBS buffer (pH 7.6, 0.05% Triton X-100) and incubated at room temperature for 15

min. After removal of the buffer, the samples were incubated for 30 min in the dark at 37°C for Cy3-tyramide signal amplification. Filters were then observed under epifluorescence microscopy.

Viral abundance and production. Viral abundance was determined by epifluorescence microscopy after extraction of viruses from the sediment using pyrophosphate (final concentration, 5 mM), sonication, and staining by SYBR Green I (*5*, *37*). Viral production was determined by time-course experiments of sediment samples previously diluted with virus-free seawater (0.02 µm pre-filtered), collected at the sediment-water interface of each benthic site (*5*, *38*, *39*). A standard dilution of sediment samples with virus-free seawater was used (sediment to virus-free seawater 1:10 vol:vol) (*5*, *38*, *39*). Replicate samples (n=3) for viral counts were collected immediately after dilution of the sediments and after 1-3, 3-6 and 12 h of incubation in the dark at in-situ temperature. Subsamples were then analyzed as reported for the determination of viral abundance. In all of the samples, the viral production was determined from linear regression analyses of the increase of viral abundances versus time.

Recovery of extracellular DNA. The extracellular DNA was recovered from sediment samples collected at each time interval of incubation by using a specific procedure previously developed (*40*). As following described, this method is based on gentle sediment washings using isotonic solution of sodium phosphate buffer supplemented with polyvinylpolypyrrolidone and low SDS concentrations, allowing avoiding cell lysis during the procedure thus selectively purifying extracellular DNA free of intracellular DNA (*39*). Briefly, sediment samples were treated with acid-washed polyvinylpolypyrrolidone (0.05% final concentration) and sodium dodecyl sulfate (final concentration, 0.1%). Then the samples were chilled on ice, centrifuged, and the supernatants were transferred to sterile tubes. The sediment pellets were washed again with sodium phosphate buffer (pH 8.0) and centrifuged. Supernatants were

combined and centrifuged for 20 min at 10000 ×g (4°C). After centrifugation, the supernatants containing extracellular DNA were filtered through 0.02-µm-pore-size filters to eliminate any contaminating viruses or prokaryotic cells. Aliquots of the supernatant were checked using epifluorescence microscopy as described above, to exclude for viral or prokaryotic contamination of the supernatant fluid after filtration. The extracellular DNA contained in the supernatant was recovered by adding 1 volume of cetyltrimethylammonium bromide solution (1% CTAB in 50 mM, Tris 10 mM EDTA, pH 8.0) and further precipitation after incubation at 65°C for 30 min, cooling on ice and centrifugation at 10000 ×g for 15 min at 4°C. The pellet was suspended in high-salt TE buffer (10 mM Tris-HCl, 0.1 mM EDTA, 1 M NaCl; pH 8.0) added to 0.6 volumes of cold isopropanol, incubated for 2 hours at -20°C and centrifuged at 10000 ×g for 15 min at 4°C. The pellets containing the DNA were suspended in MilliQ water and purified using the Wizard PCR clean-up system (Promega). The bacterial and archaeal 16*S* rDNA sequences contained within the extracellular DNA were analyzed by real-time qPCR analyses and high-throughput sequencing, as reported below.

Real-time qPCR analyses. The quantification of archaeal and bacterial 16*S* rRNA genes contained within the extracellular DNA was performed using primers and probes selectively targeting Archaea (forward primer 5'-GYGCASCAGKCGMGAAW-3', reverse primer: 5'-GGACTACVSGGGTATCTAAT-3', probe 5'-TGYCAGCCGCCGCGGTAAHACCVGC-3') (*41*) or Bacteria (forward primer: 5'-TCCTACGGGAGGCAGCAGT-3', reverse primer: 5'-GGACTACCAGGGTATCTAATCCTGTT-3', probe: 5'-CGTATTACCGCGGCTGCTGGCAC-3') (*42*). Hydrolysis probes for qPCR TaqMan assay contained a fluorescent reporter dye (6-FAM) in 5', and a Black Hole Quencher 1 (BHQ-1) in the 3' position. The amplification reactions were performed in a final volume of 15 µl in film-sealed optical 96-well qPCR plates. Each reaction contained the iQ

Supermix (Biorad), 0.8/0.2 µM (for archaeal) or 0.1/0.1 µM (for bacterial) primers/probes, respectively, and 1 µl of template DNA. According to the standard MIQE guidelines for best practice in qPCR analyses (*54*), calibration curves were included in all reactions, with a five log10 linear dynamic range, from 2.5 $\times 10^{-1}$ to 2.5 $\times 10^{-5}$ pg of template 16*S* rDNA from *E. coli* (for Bacteria) or *M. jannaschii* (for Archaea). The limit of detection of the assay was *ca.* 25 and 30 16*S* rRNA gene copies per reaction, for Bacteria and Archaea, respectively. To test for possible inhibition of qPCR, reactions were run in triplicate, using undiluted aliquots of extracellular DNA obtained from the different sediment samples, in addition to running all sample extracts in serial 10-fold dilutions. The log-linear relationship between Cq and the dilution factor was obtained in all of the samples by using the 10-fold dilution, allowing us to exclude possible bias due to qPCR inhibition (*55*, *56*). The optimal concentration of primers and probes and the thermal cycles were set following temperature and primer/probe concentration gradient tests. The adopted thermal cycling conditions were: 3 minutes at 95°C, followed by 40 cycles of 15 sec 95°C, 1 minute, 60°C for Bacteria; 3 minutes at 95°C, followed by 40 cycles of 15 sec, 95°C, 5 min 57°C for Archaea. The presence of a single PCR product of the expected length size was checked using 1% agarose gel electrophoresis. The iQ5 Optical System 2.1 Software was used to calculate Cq, efficiency (E) and R^2 values for each reaction. Results from qPCR runs were used in this study if E >98% and <102%, and R^2>0.99 (even more stringent than MIQE guidelines; (*54*)), and samples from the same incubation experiment were always analysed within the same qPCR run, thus ensuring technical consistency. All samples, standards, and negative controls were analysed in triplicate qPCR reactions. Any run for which negative controls were positive were excluded and conducted again.

High-throughput sequencing of 16*S* rRNA genes contained in the extracellular DNA pools. The bacterial and archaeal 16*S* rRNA genes contained within the extracellular DNA pools were amplified

using primer sets S-D-Bact-0341-b-S-17 (5'-CCTACGGGNGGCWGCAG-3') and S-D-Bact-0785-a-A-21 (5'-GACTACHVGGGTATCTAATCC-3') for bacteria, and S-D-Arch-0519-a-S-15 (5'-CAGCMGCCGCGGTAA-3') and S-D-Arch-1041-a-A-18 (5'-GGCCATGCACCWCCTCTC-3') for archaea (*30*). Four independent PCR analyses were carried out from each DNA sample, then the PCR products were pooled and sequenced by 454 FLX Titanium platform. Raw sequences of 16Sr DNA of bacteria and archaea were first processed to remove tags by using the TagCleaner tool (*57*). The PrinSeq tool was then used to remove sequencing artefacts, low-quality sequences (<35 on average on a sliding window of 50 bp) (*58*) and sequences shorter than 250 bp (*59*). Chimaeras were removed using the 454 SOP for Mothur (*60*). Annotation was performed using MG-RAST (*61*) with the Representative Hit Classification system (E-value 10^{-4}, cutoff identity 95%, min. alignment 100 bp). The 16*S* rDNA sequences were analyzed by normalizing to the same number (at the lowest number of sequences obtained at each site) by using the Mothur command sub.sample (*60*) without replacement; and then they were merged and clustered at 97% of similarity by using the cluster_fast algorithm contained within the USEARCH pipeline (*62*). Clusters contributing for less than 1% of the total sequences were not considered for further analyses. To generate the dendrogram on the basis of the similarity amongst the 16*S* rDNA sequences of each cluster belonging to Marine Group I Thaumarchaeota, the sequences were aligned using MUSCLE (*63*), with a regular computation mode, and the tree was constructed by using PhyML (*64*) with F84 substitution model, parsimony criteria and best of NNI and SPR topology search modes, supported by 100 bootstrap replicate analysis.

Viral diversity. Viruses were extracted from sediments using a physical-chemical procedure (*50*). Briefly, an equal volume of virus-free seawater (pre-filtered through 0.02-μm-pore-size filters) containing tetrasodium pyrophosphate (5 mM) was added to the sediment and samples were incubated in

the dark for 15 minutes and sonicated. Then, samples were shaken manually for 1 min and the supernatant was collected after centrifugation (800 ×g, 1 min). The sediments were washed once again with virus-free seawater, manually shaken for 1 min and then centrifuged (800 ×g; 1 min). Supernatants were pooled together and treated with DNase I (2U ml^{-1}) for 15 min. at room temperature. Supernatants were filtered onto 0.2-µm-pore-size filters to remove residual sediment particles and prokaryotic cells. Absence of contamination of the filtered supernatants due to bacterial and archaeal cells was routinely checked by epifluorescence microscopy countings as previously described. Then, the supernatants were filtered onto 0.02-µm-pore-size filters. This procedure allowed us to recover about 70-80% of viral particles from the sediments (calculated on the basis of viruses cumulatively recovered using four extraction steps) (*50*). Approaches based on tangential flow filtration (*65*) to concentrate viruses provided a lower recovery efficiency (16-38%) and were thus excluded.

Viral DNA was extracted and purified according to standard protocols previously described (*66*), then quantified fluorometrically (NanoDrop 3300) using SYBR Green I and sequenced on a 454 FLX Titanium platform. The quality of reads obtained was checked using the tools provided by the MG-RAST server prior to annotation (*61*). Viral sequences were analysed using MetaVir (E-value cutoff of 10^{-3} and raw reads hit ratios) (*67*). Further analyses to increase the reference database of archaeal virus genomes, included all the missing viruses known to infect archaea and lacking in publicly available reference databases. The GAAS metagenomic tool (E-value cutoff of 10^{-3}, 80% similarity) (*68*) was used to compare our sequences to archaeal viruses. The sequences contained in the viromes were first normalised to the same number by using the Mothur command sub.sample (*60*); then they were searched by tBLASTX (E-value cutoff of 10^{-3}, >50% similarity) against the reference database of archaeal virus genomes including all the missing viruses known to infect archaea and the two putative thaumarchaeal

viruses known to date and lacking in public reference databases (*27*, *28*). The tBLASTX profiles of the abundances of the DNA sequences affiliated to the different archaeal viruses obtained before and after the lysis of archaeal cells were compared. Such a comparison was done using the statistical package within the STAMP program (*69*), applying Fisher's exact test, Newcombe-Wilson method for calculating confidence intervals (CIs, 95%) and Storey FDR multiple test correction.

Archaeal and bacterial diversity. The DNA associated with microbial components (i.e. intracellular DNA) was recovered from sediment samples following specific procedures previously developed (*40*). The bacterial and archaeal16*S* rRNA genes contained within the intracellular DNA pools were amplified and analyzed by high-throughput sequencing, as previously described for the analysis of the extracellular DNA. Moreover, the intracellular and extracellular DNA pools were directly sequenced by 454 FLX Titanium platform to compare bacterial and archaeal sequences contained within these two metagenomes. The similarity between bacterial and archaeal diversity in intracellular and extracellular DNA pools was assessed using the statistical package available in Primer 6+ software (*70*).

Heterotrophic and chemoautotrophic C production of bacteria and archaea and effect of the viral shunt on chemoautotrophy. To identify the relative contribution of bacteria versus archaea in heterotrophic and chemoautotrophic C production, parallel experiments were conducted on untreated sediment samples and samples treated with N1-guanyl-1.7-diaminoheptane (GC7) (*22*, *45*, *46*) to selectively inhibit archaeal metabolism. For heterotrophic C production determinations, sediment sub-samples were added with 0.2-µm-pre-filtered seawater, containing (^{3}H)-leucine (68 Ci mmol^{-1}; final 0.5-1.0 µM). Samples were then incubated in the dark and at the in situ temperatures. Time-course experiments over 6 h and concentration-dependent incorporation experiments (from 0.05 µM to 5.0 µM

leucine) were also carried out to define the linearity and the saturation level of the (^{3}H)-leucine incorporation, respectively. Additional replicate sediment sub-samples were added with 1 mM GC7 before (^{3}H)-leucine addition. Blanks (n=3) for each sediment sample were added with ethanol immediately before (^{3}H)-leucine addition. After incubation, samples were supplemented with ethanol (80%), centrifuged, washed again two times with ethanol (80%), and the sediment was finally re-suspended in ethanol (80%) and filtered onto polycarbonate filters (0.2 µm pore size; vacuum <100 mm Hg). Subsequently, each filter was washed four times with 2 ml of 5% TCA, then transferred into a Pyrex tube containing 2 ml of NaOH (2M) and incubated for 2 h at 100°C. After centrifugation at 800 ×g, 1 ml of supernatant fluid was transferred to vials containing an appropriate scintillation liquid. The incorporated radioactivity in the sediment samples was measured with a liquid scintillation counter. The prokaryotic heterotrophic C production was calculated as follows:

$$\text{Prokaryotic heterotrophic C production} = \text{LI} \times 131.2 \times (\%\text{Leu})^{-1} \times (\text{C/protein}) \times \text{ID}$$

where: LI is the leucine incorporation rate (mol g^{-1} h^{-1}), 131.2 is the molecular weight of leucine, %Leu is the fraction of leucine in a protein (0.073), C/protein is the ratio of cellular carbon to protein (0.86), and ID is the isotope dilution, assuming a value of 2.

For chemoautotrophic C production determinations, sediment sub-samples were added with 0.2-µm-pre-filtered seawater (collected at the sediment-water interface of each station) containing (^{14}C)-bicarbonate (58 mCi $mmol^{-1}$; final 12 µCi ml^{-1}) (*22*). Samples were incubated in the dark at in situ temperature for 6 h to 8 h. The incubation time was selected on the basis of time-course experiments of (^{14}C)-bicarbonate incorporation carried out over 48 h. Additional replicate sediment sub-samples were added with 1 mM

GC7 before (^{14}C)-bicarbonate addition. After incubations, C incorporation in all samples was stopped with the addition of 0.2-µm prefiltered formaldehyde solution (final concentration, 2%). Blanks were added with 0.2-µm prefiltered formaldehyde solution immediately prior to the (^{14}C)-bicarbonate addition. Samples were subjected to three washes with PBS and centrifugation at 13500× g for 10 min. After removal of the final supernatant fluid, the samples were incubated overnight in 1N HCl. After this incubation, samples were added with 10 ml scintillation liquid, mixed, centrifuged (3000 ×g, 10 min), and the supernatants were transferred into vials for the quantification by liquid scintillation counter (Packard Tri-Carb). The nonspecific binding of (^{14}C)-bicarbonate to the sediments was taken into account by analyzing the (^{14}C) radioactivity of formaldehyde-treated sediment sub-samples or pre-combusted in a muffle furnace before (^{14}C)-bicarbonate addition. The following formula was used to convert the radioactivity in the samples (as disintegration per minute; DPM) into inorganic C incorporated per g dry sediment (60°C, 24 h) per h:

$$\text{Chemoautotrophic C production} = \text{DPMinc} \times 12 \times 1.05 \times \text{DIC} \times (\text{S.A.} \times 2.22 \times 10^{12} \times \text{Y} \times \text{g} \times \text{H})^{-1}$$

where: DPMinc is the difference between the DPM in the sample and the DPM in the sediment blanks; 12 is the atomic weight of C; 1.05 is the isotope coefficient used for correcting the uptake of (^{14}C) (uptake of ^{14}C is 5% lower than the uptake of ^{12}C); DIC is the dissolved inorganic C concentration (molarity) estimated from the alkalinity determined in the bottom seawater used for the incubation experiments of the sediment samples; S.A. is the specific activity of the (^{14}C)-bicarbonate (Ci mol^{-1}); 2.22×10^{12} is the DPM emitted by 1 Ci; Y is the concentration of added (^{14}C)-bicarbonate (molarity); g is the mass of sediment expressed as dry weight; H is the incubation time (hours).

To provide information on the contribution of the virus-mediated organic matter release and its subsequent utilization through heterotrophic metabolism, we estimated the mole N released through viral lysis from the mole C released, based on a theoretical archaea and bacteria C:N content ratio of 4 and assuming all this N to be recycled through heterotrophic metabolism to ammonia available for archaeal chemoautotrophs. The mole N required by archaea were calculated multiplying the mole CO_2 fixed by archaea (based on radiotracers experiments) by 10 (considering 1 mole C fixed each 10 mole N oxidized). The resulting mole N supplied through viral lysis and subsequent heterotrophic recycling of the organic matter released were used to calculate the contribution to the total N requirement of archaea.

Statistical analyses. For the experiments of viral production using the dilution approach as described above, the differences in viral abundance over time were tested by one-way analysis of variance (ANOVA) followed by pair-wise test. These statistical analyses indicated that in all samples viral abundances increased significantly from the beginning of the experiments to 6-12 h. To test for differences in the viral abundance, in the viral production rates and in the number of bacterial or archaeal 16*S* rRNA gene copies over time during incubation experiments of samples treated with inhibitors of bacterial and archaeal metabolism, two-way analysis of variance (ANOVA) was carried out, followed by pairwise tests. Finally, one-way analysis of variance was conducted to test for differences in the virus-induced mortality of bacteria and of archaea.

Supplementary Figures and Tables

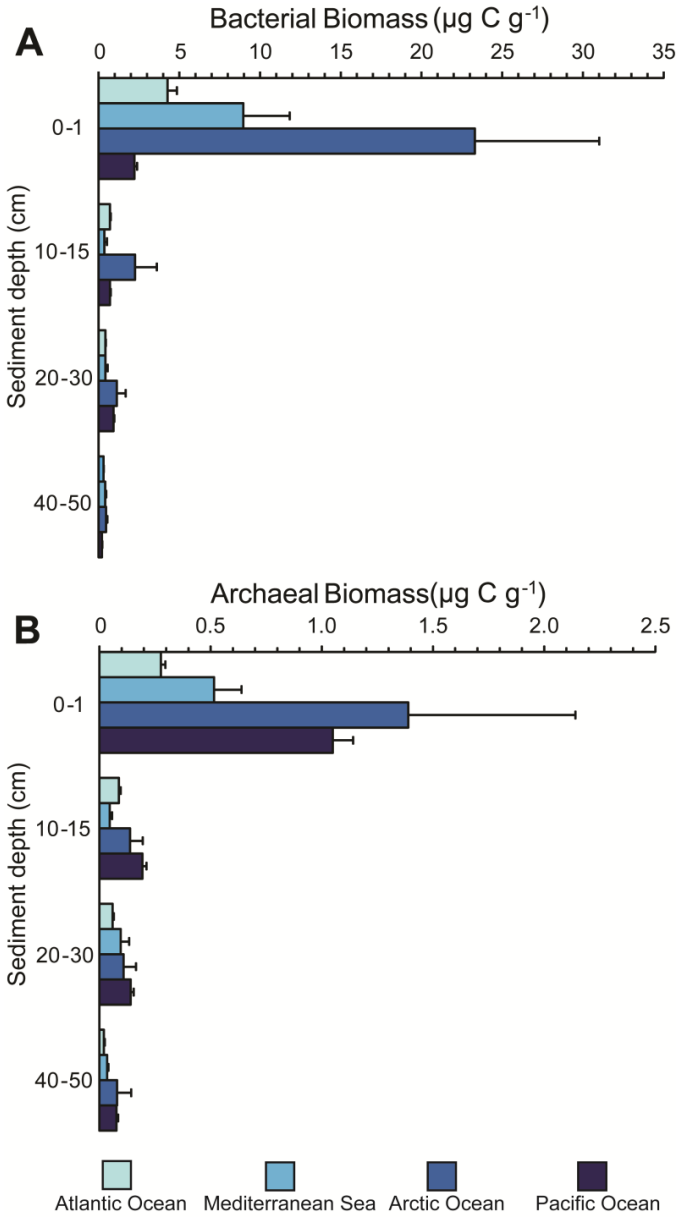

fig. S1. Bacterial and archaeal biomass in deep-sea sediments. Vertical patterns of bacterial (**A**) and archaeal (**B**) biomass from the surface (top 1 cm) down to 50-cm sediment depth (at intervals of 0-1, 10-15 20-30 and 40-50-cm depth). Reported are average values and standard deviations of deep-sea sediments collected from Arctic, Atlantic and Pacific Oceans and Mediterranean Sea.

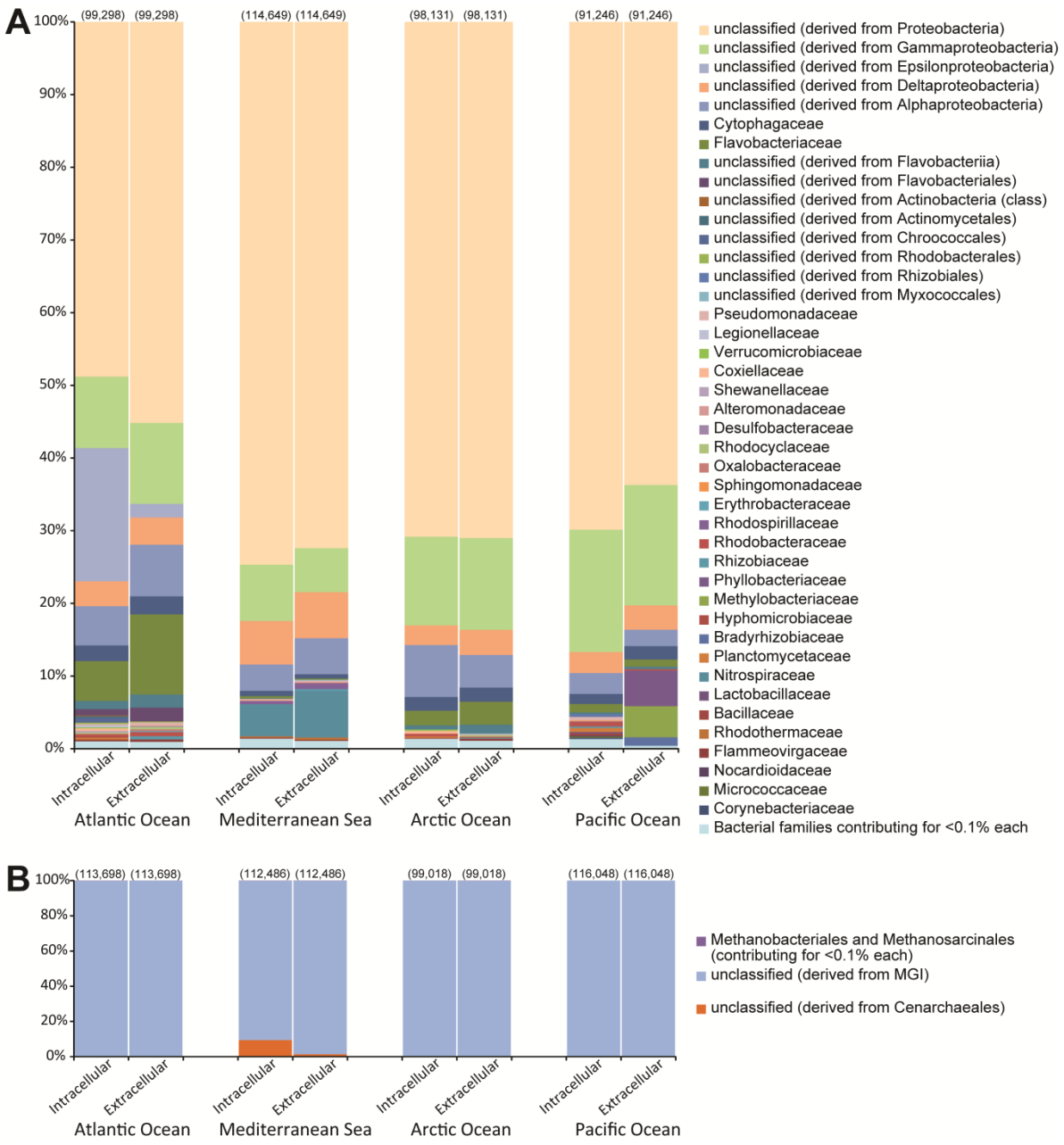

fig. S2. Diversity of bacterial and archaeal 16*S* rRNA genes in deep-sea sediments. Contribution of 16*S* rDNA sequences belonging to different bacterial (**A**) and archaeal (**B**) taxa to the total number of sequences in the intracellular and extracellular DNA pools. To compare intracellular and extracellular DNA pools the 16*S* rDNA sequences were normalised to the same number (at the lowest number of

sequences obtained at each site by randomly sub-sampling the sequences contained in the sample with the highest number), which is reported in brackets.

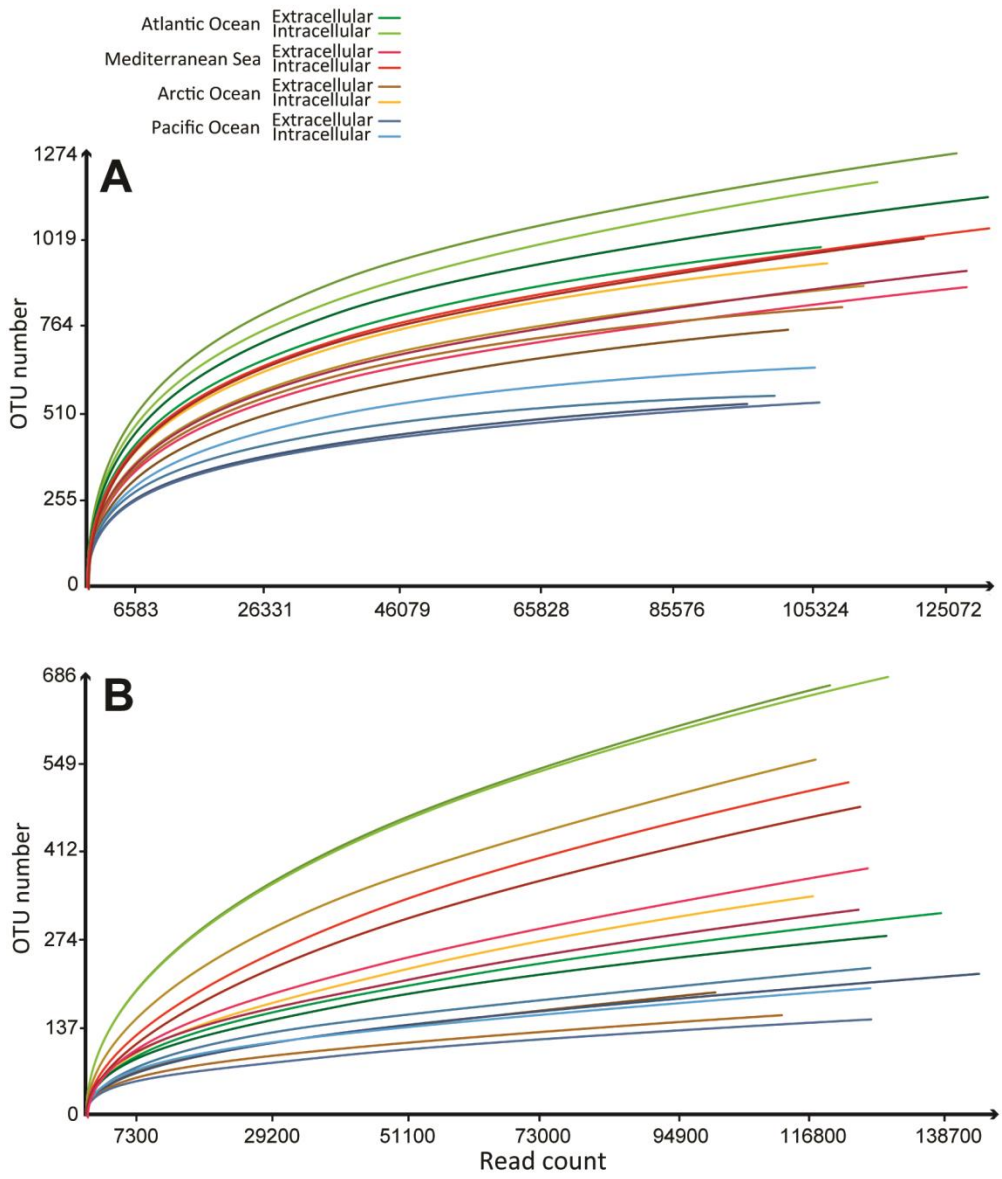

fig. S3. Rarefaction curves. Reported are the rarefaction curves of bacteria (**A**) and archaea (**B**) for the samples analysed through 16*S* rRNA gene pyrosequencing.

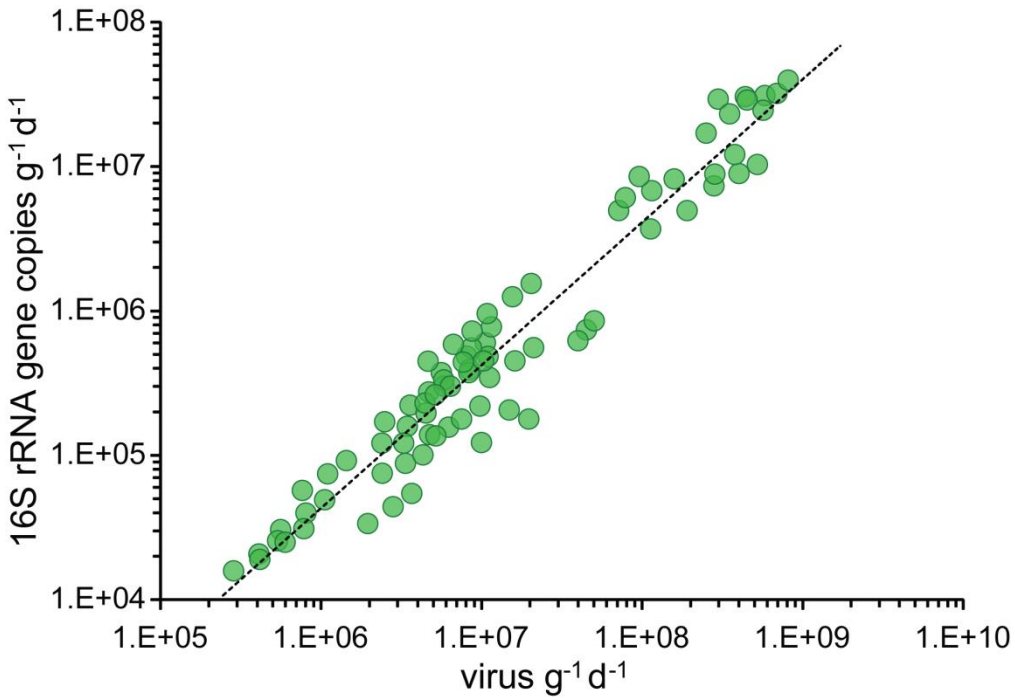

fig. S4. Rates of lytic infections versus 16*S* rRNA genes released from lysed hosts. The figure shows the relationship between the rates of viral production (x axis) and the total 16*S* rRNA genes (as the sum of bacterial and archaeal 16*S* rRNA genes, y axis) released from the lysed cells into the extracellular DNA pools ($Y = 0.0474x + 7.38\times10^{4}$; $R^2 = 0.863$; n=84; $p<0.01$).

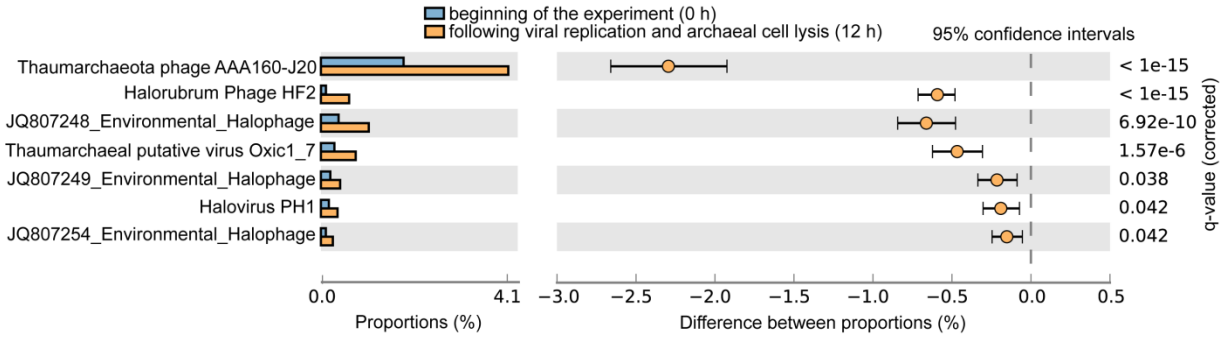

fig. S5. Viruses responsible for archaeal mortality identified by metagenomics. The left panel shows the change in the relative abundances of the DNA sequences affiliated to different archaeal viruses, including currently known thaumarchaeal viruses (*27*, *28*), contained in the viromes analysed at the beginning of the time-course experiments (light blue bars) and after 12 h (i.e., after the lysis of archaeal cells, orange bars). The right panel shows the output of statistical analysis which highlights the significant increase in the relative abundances of the DNA sequences affiliated to different archaeal viruses after 12 h.

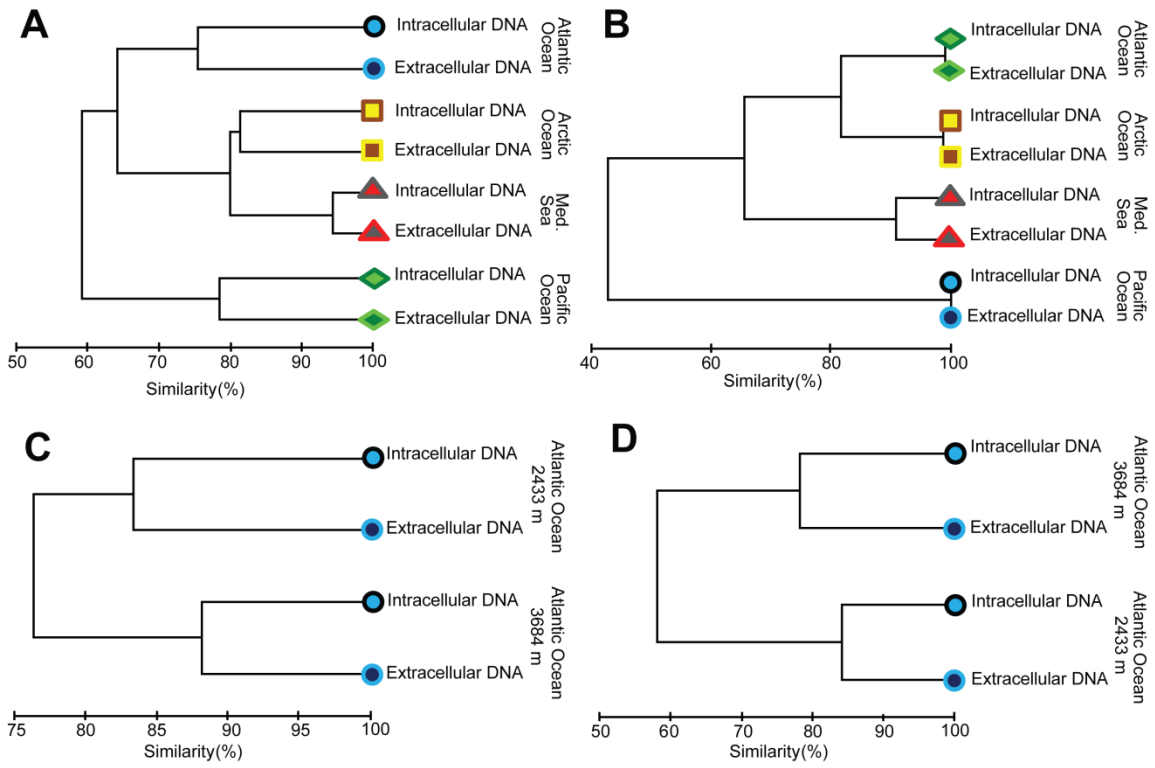

fig. S6. Similarity between bacterial and archaeal assemblage composition in intracellular and extracellular DNA pools. Outputs of the cluster analysis, based on Bray-Curtis similarity, carried out on bacterial (**A**) and archaeal (**B**) 16*S* rDNA sequences in the intracellular and extracellular DNA pools and on bacterial (**C**) and archaeal (**D**) sequences contained within the two metagenomes (i.e., intracellular and extracellular DNA pools analysed by direct pyrosequencing).

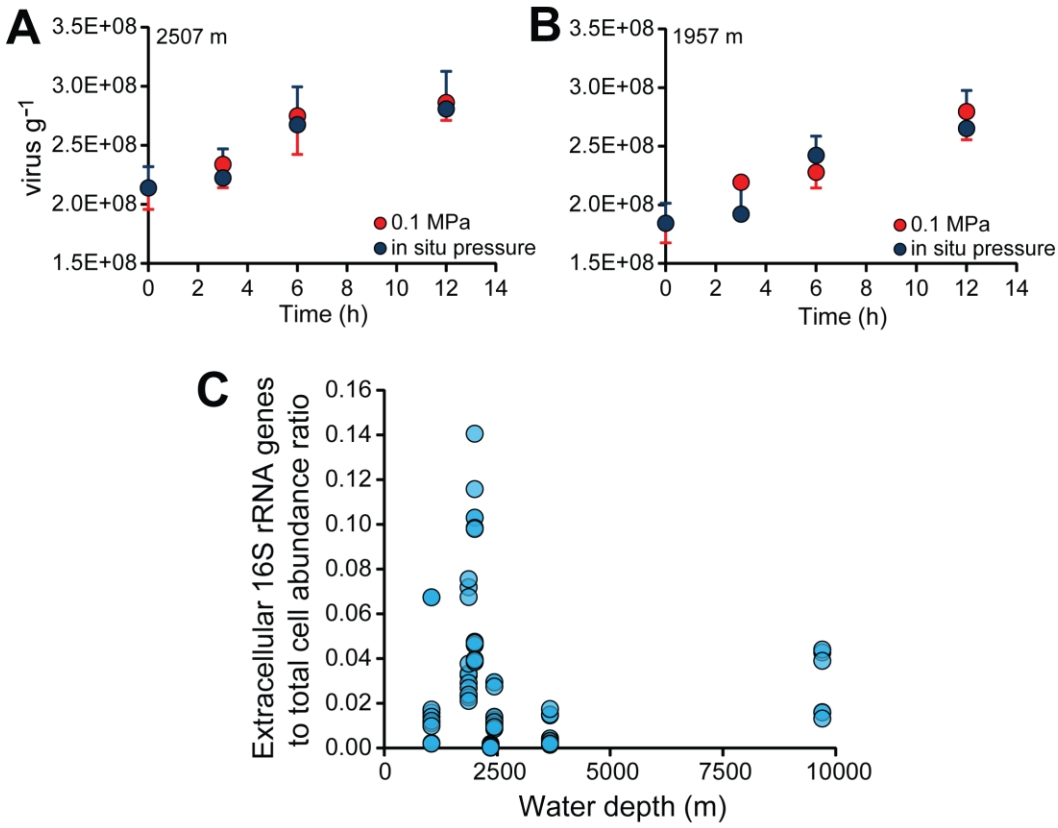

fig. S7. Effect of pressure on viral production, DNA release, and cell burst. Reported are the results of the analyses of the effects of pressure (i.e., decompression vs in situ pressure) on: (**A**, **B**) viral production determined by the dilution method for deep-sea sediments collected from the Mediterranean Sea, and (**C**) the ratio of copy number of 16*S* rRNA genes contained in the extracellular DNA to the total cell abundance determined in the deep-sea sediments collected in the stations analysed in the present study. All graphs reported above indicate that decompression had no significant effects on the viral production, burst of cells and release of 16*S* rRNA genes in the environment.

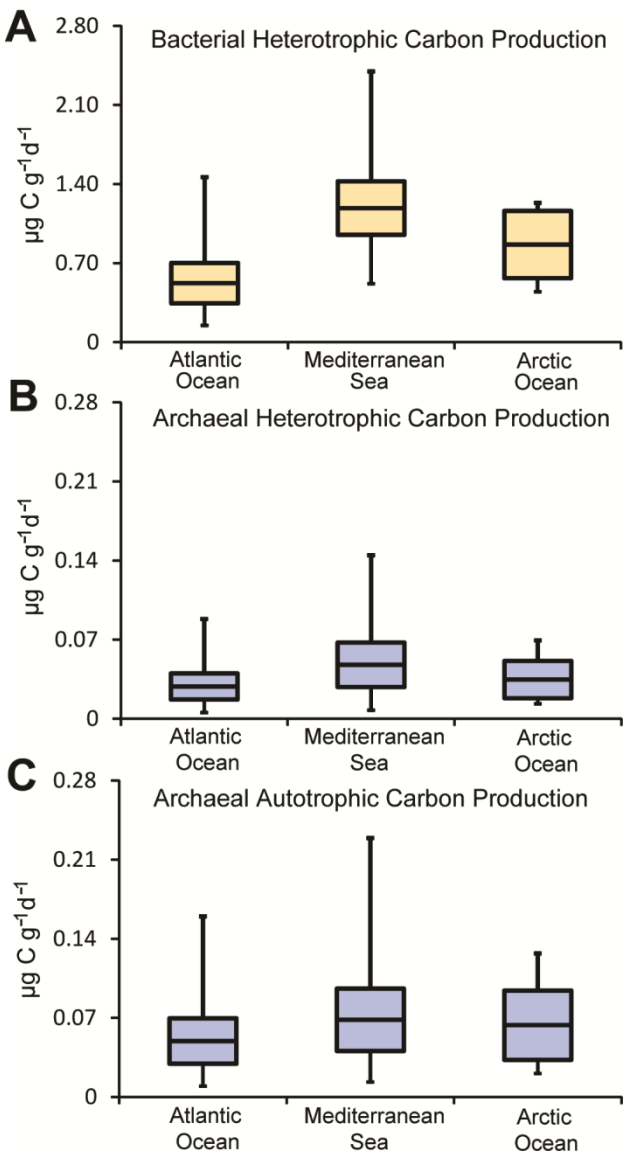

fig. S8. Heterotrophic and chemoautotrophic C production. Reported are the values of heterotrophic and chemoautotrophic C production in the different oceanic regions investigated. Chemoautotrophic production was almost entirely due to archaea since no incorporation of (^{14}C)-bicarbonate was observed after the addition of the inhibitor of the archaeal metabolism (GC7). Since both bacteria and archaea contributed to heterotrophic C production, the values of heterotrophic C production of each component were calculated by difference between total heterotrophic C production and values measured after the inhibition of the archaeal metabolism (i.e., addition of GC7).

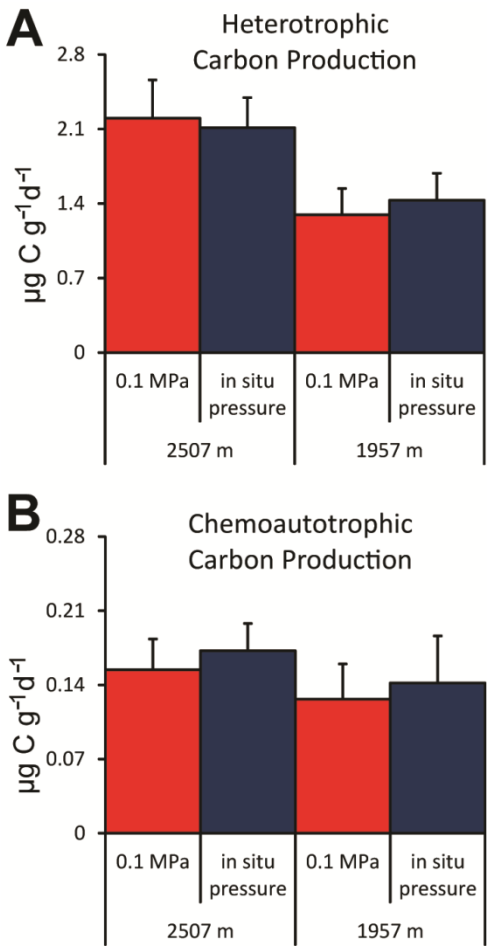

fig. S9. Effect of pressure on C production. Comparison of rates of heterotrophic (**A**) and chemoautotrophic C production (**B**) for deep-sea sediments collected from the Mediterranean Sea, as measured at in situ pressure and at 0.1 MPa.

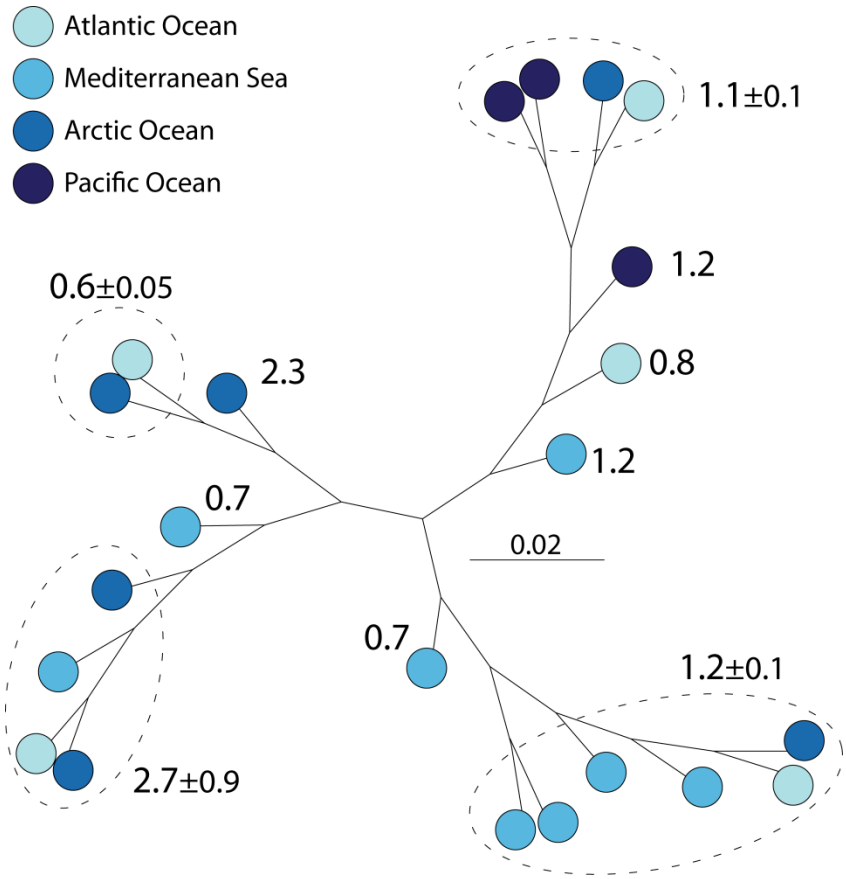

fig. S10. Impact of viruses on MG-I Thaumarchaeota in surface deep-sea sediments. Reported is the dendrogram showing the diversity of clusters of MG-I Thaumarchaeota (determined on the basis of 16*S* rDNA sequence similarity), in relation with the respective impact of viruses. The colours indicate the different deep-sea regions investigated. The numbers represent the relative impact of viral infection on each cluster, determined based on the increased number of 16*S* rDNA sequences in the extracellular DNA pool during time-course experiments. The scale bar indicates the expected substitutions per site.

table S1. Details on the deep-sea sampling areas investigated. Reported are: oceanographic region, latitude, longitude, sampling depth, sampling period, sediment sampling device, bottom water temperature (T), salinity and biopolymeric carbon (BPC, expressed as mg C g^{-1} sediment dry weight) concentrations in the top 1 cm of sediment. Concentrations of BPC (calculated as the sum of the C equivalents of protein, carbohydrate and lipid concentrations) in deep-sea sediments has been used as a proxy of food availability for benthic consumers (*71*).

Oceanographic region	**Latitude (°N)**	**Longitude (°E)**	**Sampling depth (m)**	**Sampling period**	**Sampling device**	**T (°C)**	**Salinity**	**BPC (mg C g^{-1})**
Atlantic Ocean	48.154	-10.560	3668	June 2009	Multicorer	2.4	34.9	2.11± 0.23
Atlantic Ocean	48.684	-11.201	2433	June 2009	Multicorer	2.8	35.0	2.42±0.31
Mediterranean Sea	42.033	4.699	2348	October 2009	Multicorer	12.9	38.5	1.78 ± 0.09
Mediterranean Sea	42.214	4.257	1863	October 2009	Multicorer	12.9	38.5	0.85 ± 0.05
Mediterranean Sea	42.016	5.542	2507	March 2011	Multicorer	12.9	38.5	2.62 ± 0.37
Mediterranean Sea	42.199	4.418	1957	March 2011	Multicorer	12.9	38.5	1.43 ± 0.24
Arctic Ocean	76.264	13.571	1040	July 2010	Multicorer	-0.5	34.9	1.99 ± 0.10
Arctic Ocean	77.149	9.324	2000	July 2010	Multicorer	-0.5	34.9	3.17 ± 0.63
Pacific Ocean	29.09	142.481	9776	December 2011	ROV (ABISMO)	2.26	34.7	1.98 ± 0.03

table S2. Output of the in silico analyses dealing with the specificity and the coverage of oligonucleotides targeting 16*S* rRNA used in the present study. For each primer or probe, shown is the comparison between the values reported in 2013 (*30*) and values obtained using the updated SILVA database (2015). The coverage with 1 mismatch is reported in bracket. n.a.= not available.

Common name	**Sequence 5'-3'**	**Coverage**					
		Archaea		**Bacteria**		**Eukaryota**	
		2013	**Updated 2015**	**2013**	**Updated 2015**	**2013**	**Updated 2015**
Arch349F	GYGCASCAGKCGMGAAW	79.6(92.4)	80.3(93.1)	0(0)	0(0)	0(0.1)	0(0.1)
A806R	GGACTACVSGGGTATCTAAT	87.4(96.5)	87.2(96.2)	7.8(92.1)	8.0(91.7)	0(0.1)	0(0.1)
Bact806R	GGACTACCAGGGTATCTAATCCTGTT	0.1(0.2)	0.1(0.1)	78.6(82.6)	78.5(83.4)	0(0)	0(0)
Bact340F	TCCTACGGGAGGCAGCAGT	0(0.3)	0(0.2)	89.4(95.0)	88.7(94.8)	0(0)	0(0)
Arch516F	TGYCAGCCGCCGCGGTAAHACCVGC	81.5(95.3)	83.9(95.7)	0(0)	0(0)	0(1.2)	0(1.4)
Bac probe	CGTATTACCGCGGCTGCTGGCAC	n.a.	0(0.4)	n.a.	78.4(95.6)	n.a.	0(1.0)
EUB-338-I	GCTGCCTCCCGTAGGAGT	0(0)	0(0)	90.9(95.2)	90.4(95.1)	0.0	0(0.1)
EUB-II	GCAGCCACCCGTAGGTGT	n.a.	0(0)	n.a.	0.8(2.3)	n.a.	0(0)
EUB-III	GCTGCCACCCGTAGGTGT	n.a.	0(0)	n.a.	1.5(2.4)	n.a.	0(0.1)
Arch915R	GTGCTCCCCCGCCAATTCCT	78.4(86.7)	83.2(91.5)	0(0)	0(0)	0(0)	0(0)
A519F	CAGCMGCCGCGGTAA	95.2(9.7)	95.3(97.8)	95.7(98.4)	94.3(97.9)	92.7(97.2)	92.8(97.3)
Arch1017R	GGCCATGCACCWCCTCTC	79.8(95.2)	80.7(95.0)	0(0)	0(0)	0(0)	0(0)
Bact 805R	GACTACHVGGGTATCTAATCC	90.1(96.5)	89.7(96.1)	90.4(96.2)	90.1(96.3)	0(0.8)	0(0.8)
Bact 341F	CCTACGGGNGGCWGCAG	0.5(66.6)	0.7(67.3)	94.9(98.1)	94.4(97.8)	0(0.2)	0.1(0.2)

table S3. Number of 16*S* rDNA sequences obtained before and after the cleaning process. Reported is the number of sequences obtained by 454 pyrosequencing of bacterial and archaeal 16*S* rRNA genes contained within the extracellular and intracellular DNA pools collected at the different sampling sites.

DNA sample	Sampling depth (m)	Number of raw sequences	Number of sequences after cleaning
Atlantic Ocean, Intracellular DNA, Archaea, before viral infection	2433	159907	120079
Atlantic Ocean, Extracellular DNA, Archaea, before viral infection		170184	133900
Atlantic Ocean, Extracellular DNA, Archaea, after viral infection		167589	125418
Atlantic Ocean, Intracellular DNA, Bacteria, before viral infection		157829	110265
Atlantic Ocean, Extracellular DNA, Bacteria, before viral infection		134664	99298
Atlantic Ocean, Extracellular DNA, Bacteria, after viral infection		167596	124870
Mediterranean Sea, Intracellular DNA, Archaea, before viral infection	2348	156992	112486
Mediterranean Sea, Extracellular DNA, Archaea, before viral infection		163182	118498
Mediterranean Sea, Extracellular DNA, Archaea, after viral infection		172914	121539
Mediterranean Sea, Intracellular DNA, Bacteria, before viral infection		176771	122737
Mediterranean Sea, Extracellular DNA, Bacteria, before viral infection		175070	119174
Mediterranean Sea, Extracellular DNA, Bacteria, after viral infection		171714	119778
Arctic Ocean, Intracellular DNA, Archaea, before viral infection	2000	152861	113975
Arctic Ocean, Extracellular DNA, Archaea, before viral infection		149525	105441
Arctic Ocean, Extracellular DNA, Archaea, after viral infection		143962	99018
Arctic Ocean, Intracellular DNA, Bacteria, before viral infection		144983	102049
Arctic Ocean, Extracellular DNA, Bacteria, before viral infection		153142	105429
Arctic Ocean, Extracellular DNA, Bacteria, after viral infection		149220	98131
Pacific Ocean, Intracellular DNA, Archaea, before viral infection	9776	149557	121067
Pacific Ocean, Extracellular DNA, Archaea, before viral infection		151487	116048
Pacific Ocean, Extracellular DNA, Archaea, after viral infection		171877	133933
Pacific Ocean, Intracellular DNA, Bacteria, before viral infection		145561	101221
Pacific Ocean, Extracellular DNA, Bacteria, before viral infection		144703	101376
Pacific Ocean, Extracellular DNA, Bacteria, after viral infection		139142	91246

table S4. Output of the statistical tests for the experiments of inhibition of bacterial and archaeal metabolism. Reported is the output of the two-way analysis of variance to test for differences in the abundance of viruses and in the number of bacterial and archaeal 16*S* rRNA gene copies during incubations (start, T0h, and end, T12h) of samples treated with bacterial and archaeal metabolism inhibitors and of not treated samples (i.e., controls) (see fig. 3 in the main text). Reported are the results of the main tests and those of the post-hoc pairwise comparisons. Significant differences are indicated with asterisks (*, $p<0.05$; **, $p<0.01$); ns, indicating no statistical significance.

		Source	SS	F	p
Main test	Viral abundance	Time	415.53	4.5	*
		Treatment	2090.5	22.9	***
		Time x Treatment	1266.0	13.9	**
	Bacterial 16S rDNA	Time	1721.8	5.8	*
		Treatment	3502.2	11.7	**
		Time x Treatment	2131.6	7.1	*
	Archaeal 16S rDNA	Time	804.8	5.1	*
		Treatment	2026.9	12.9	**
		Time x Treatment	1473.4	9.4	**

		Within level 'control' (T0h vs T12h)	Within level 'treatment' (T0h vs T12h)	Within level '0h' (control vs treatment)	Within level '12h' (control vs treatment)
Pairwise test	Viral abundance	**	ns	ns	**
	Bacterial 16S rDNA	**	ns	ns	**
	Archaeal 16S rDNA	**	ns	ns	**

table S5. Output of the statistical tests for the experiments of selective inhibition of archaeal metabolism. Reported is the output of the two-way analysis of variance to test for differences in the number of bacterial and archaeal 16*S* rRNA gene copies during incubations (start, T0h, and end, T12h) of samples treated with archaeal protein synthesis inhibitor and of not treated samples (i.e., controls) (see fig. 4 in the main text). Reported are the results of the main tests and those of the post-hoc pairwise comparisons. Significant differences are indicated with asterisks (*, $p<0.05$; **, $p<0.01$; ***, $p<0.001$); ns, indicating no statistical significance.

		Source	SS	F	p
Main test	Bacterial 16S rDNA	Time	1820.2	144.3	***
		Treatment	0.5	0.1	ns
		Time x Treatment	3.2	0.3	ns
	Archaeal 16S rDNA	Time	103.8	17.1	**
		Treatment	84.4	13.9	**
		Time x Treatment	51.5	8.5	*

		Within level 'control' (T0h vs T12h)	Within level 'treatment' (T0h vs T12h)	Within level '0h' (control vs treatment)	Within level '12h' (control vs treatment)
Pairwise test	Bacterial 16S rDNA	***	**	ns	ns
	Archaeal 16S rDNA	**	ns	ns	**

table S6. Details on ^{14}C analyses. Reported is the comparison of values of ^{14}C (expressed as disintegration per minute g^{-1} h^{-1}) of formalin-treated and untreated sediments analyzed in the different sampling sites of the different oceanographic regions. Reported are also the values for sediment samples added with GC7 to inhibit archaeal metabolism.

Oceanographic region	Sampling depth (m)	Treatment	DPM g^{-1} h^{-1}
Atlantic Ocean	3668	Formalin-treated	181 ± 16
		GC7-added	198 ± 20
		Untreated	688 ± 43
Atlantic Ocean	2433	Formalin-treated	897 ± 51
		GC7-added	79 ± 69
		Untreated	6987 ± 1603
Mediterranean Sea	2348	Formalin-treated	112 ± 25
		GC7-added	135 ± 32
		Untreated	988 ± 74
Mediterranean Sea	1863	Formalin-treated	160 ± 29
		GC7-added	179 ± 28
		Untreated	852 ± 59
Mediterranean Sea	1957	Formalin-treated	432 ± 142
		GC7-added	534 ± 187
		Untreated	8725 ± 2738
Arctic Ocean	1040	Formalin-treated	184 ± 12
		GC7-added	162 ± 45
		Untreated	1914 ± 147
Arctic Ocean	2000	Formalin-treated	467 ± 31
		GC7-added	501 ± 48
		Untreated	5237 ± 1007